ISSN: 2634-9221
European Journal of Applied Sciences; Vol. 14 No. 05 (2026) (163-186)
https://doi.org/10.14738/ejas.1405.12170

Stability and Biodegradation Studies of Bioplastics Derived from Banana and Plantain Peels Doped with Particles of Egg Shell and Iron Rust

Olaoluwa Ayobami Ogunkunle[1], Oluwaseun Temitope Adeleye[1], Emmanuel Gabriel Fakola[1] and Oluwamumiyo Dorcas Adeojo[2]

1. Department of Chemistry, Faculty of Science, Obafemi Awolowo University, Ile-Ife, Osun State, Nigeria
2. Department of Chemistry, Faculty of Science, University of Ibadan, Ibadan, Oyo State, Nigeria

Abstract: Plastic pollution has emerged as a global environmental crisis due to the non-biodegradability and ecological toxicity of conventional petroleum-based plastics. In this study, bioplastics were developed using banana and plantain peels (*Musa nana*, *Musa paradisiaca*, and *Musa sapientum var paradisiaca*), which are widely available agro-wastes. These bioplastics were doped with eggshell and iron rust which are natural and renewable sources of Ca^{2+} and Fe^{3+} ions respectively to enhance their durability, mechanical strength, thermal stability, and biodegradation performance. The produced bioplastics were characterized using several techniques including elemental characterization (EDXRF), Fourier-transform infrared spectroscopy (FTIR), and scanning electron microscopy (SEM). The mechanical properties (tensile strength, Young's modulus, and elongation at break) of the bioplastics were assessed using standard methods, and water absorption and biodegradation tests were conducted to evaluate their environmental performance. The study revealed that doping with eggshell significantly increased tensile strength and Young's modulus, indicating enhanced stiffness and bonding within the polymer matrix. Iron rust, in contrast, promoted faster biodegradation and greater flexibility, albeit at the cost of reduced mechanical strength. SEM images demonstrated strong interfacial bonding and homogeneous dispersion of fillers. FTIR analysis confirmed enhanced molecular interactions and new bond formations through hydroxyl and carbonyl functional groups. Water absorption and soil burial degradation tests indicated that all bioplastics were biodegradable, with degradation rates influenced by both additive type and acid treatment concentrations. These findings demonstrate the potential of agro-waste lignocellulosic materials, additive-enhanced bioplastics as viable alternatives to conventional plastics, offering a sustainable solution to plastic waste and promoting circular bio-economy practices.

Keywords: *Banana, Bioplastics, Egg shell, Iron rust, Additives*

INTRODUCTION

Plastics are extensively used in our daily lives. Their uses range from textiles, healthcare products, automobiles, toys, packaging, and many others, making them seem like a basic necessity that the world cannot do without (George, 2020). Since the discovery of synthetic plastics, they have been employed in various applications due to their interesting properties, which include mechanical strength, durability, lightness, and low cost (Desidery & Lanotte, 2022). Despite their obvious advantages, their extensive use has created another environmental issue: plastic pollution (Ghaffar et al., 2022). Plastic pollution in the last two decades has become a significant global issue, appearing in most global summits on climate change and environmental concerns. Plastics degrade slowly and, during degradation, contribute extensively to carbon dioxide emissions while releasing other toxic substances into the environment (Ghaffar et al., 2022; Sharma et al., 2023).

In response to the environmental problems created by plastic pollution, bioplastics have emerged as potential alternatives. Bioplastics have attracted the interest of researchers and governments worldwide due to their biodegradability (Pooja et al., 2023). Interestingly, bioplastics are sourced from renewable resources in nature, including cellulose, starch, and others (Emadian et al., 2017). Bioplastics often biodegrade through the action of microorganisms, emitting carbon dioxide in minimal amounts during the process. Thus, they are environmentally friendly (Muthusamy & Pramasivam, 2019). Despite their potential to replace plastics, their limitation in terms of low mechanical strength poses a critical challenge to their usage (Folino et al., 2020; Rosenboom et al., 2022).

Banana and plantain peels, which are treated as waste in most countries, hold huge potential as raw materials for bioplastic production due to their starch content and availability (Alcivar-Gavilanes et al., 2022; Maura et al., 2024). On average, they contain 6-9% starch and are rich in dietary fiber, proteins, potassium, and essential amino acids. They have also been reported to be rich in carotenoids and polyphenols, which vary in amounts depending on the species, variety, and maturation (Ansari et al., 2023; Tsado et al., 2021). Several studies have reported the use of banana and plantain peels in producing bioplastics. For instance, Dalimunthe et al., (2024) reported the use of Kepok banana peels in the production of bioplastic spoons. The bioplastic spoons, which incorporated areca nut peel as a reinforcing agent and glycerol as a plasticizer, exhibited significant potential as substitutes for plastic spoons. Razak et al. (2024) evaluated the cellulose content of bioplastics derived from banana peel starch and tapioca. The study, which reported the potential of the bioplastic for food packaging, showed that bioplastics can withstand different conditions. Comparative tests showed that banana peel bioplastics with chemical-based additives had greater elongation at break and tensile strength compared to natural-based alternatives (Azieyanti et al., 2020). Additionally, biodegradable polymers derived from banana peels have demonstrated potential for use in planting bags; the maximum density and lowest porosity were obtained with a 40% weight concentration of banana peels (Huzaisham & Marsi, 2020). With an average weight loss of 65.1%, these bioplastics also showed better biodegradability than commercial substitutes.

a b c

Figure 1: Sources of the Experimental Samples (a) *Musa nana* (Paranta), *(b) Musa parasidsiaca* (Agbagba) *and (c) Musa sapientum var. paradisiaca* (Pambo)

Additives are crucial in the production of conventional plastics and bioplastics. They are often added to plastics to enhance their properties and performance (Gressler et al., 2020). In conventional plastics, their function is not limited to improving the manufacturing process, enhancing desired properties and providing protection from environmental factors. For bioplastics, additives such as plasticisers, fillers and cross-linking agents are added to enhance their mechanical strength, increase their thermal stability and improve their biodegradability (Abu Ubaidah et al., 2024). In recent times, studies have reported the use of egg shells as additives in the production of bioplastics. Hassan et al. (2014) reported the enhancement of the thermal stability and mechanical strength of biopolymers by incorporating egg shells based nanoparticles. Similarly, in potato starch-based bioplastics, egg shell have been reported to account for to account for increase in the tensile strength of the bioplastic by 4.94% while also accounting for reduced water absorption (by 10.95%). Interestingly in that study, egg shells performed better than chitosan as an additive for the bioplastic (Kasmuri & Zait, 2018).

Eggshells, a calcium carbonate-rich waste product, have emerged as a viable filler in polymer composites. Research indicates that adding eggshell particles into polymers can improve mechanical characteristics while reducing material costs (Homavand et al., 2024; Kumar et al., 2024). Various polymer matrices, such as polylactic acid (PLA), have been investigated with eggshell reinforcement (Homavand et al., 2024). The inclusion of an inapproriate amount of egg shell powder reduces the tensile strength and hardness while increasing elongation at break and flexural strength dues to the repulsive forces generated when the particles Ca^{2+} ions are too close to eachother (Senthil & Madan, 2015). Water absorption in these composites increases with increasing eggshell content and exposure time (Senthil & Madan, 2015).

Iron rust, a common product of corrosion, is not a common plastic additive, nevertheless iron based additives have been explored as pro-oxidants in facilitating the degradation of plastics and bioplastics. Studies by Ataeian et al. (2024) and Wang et al. (2021) reveal that they are likely to play a role in the development of plastics and bioplastics that degrade easily. These findings suggest that rust, or iron(III) oxide, could be explored as a potential additive for bioplastics to enhance their degradation. Given that iron-based additives have already shown promising in enhancing the degradation of plastics, a naturally occurring and widely available iron rust might be a cheaper and more environmentally friendly additive.

The objective of this study is to evaluate the stability and biodegradation properties of bioplastics, derived from banana and plantain peels, incorporating eggshell and iron rust particles as additives. By exploring the effects of these additives, this research seeks to enhance the mechanical properties, thermal stability, and biodegradability of the bioplastics.

METHODOLOGY

Samples Collection and Preparation

Matured but unripe banana (samples of three species (*Musa nana*, *Musa paradisiaca* and *Musa sapientum var paradisiaca*) were obtained from Tonkere village around Obafemi Awolowo University, Ile-Ife, Osun State. The banana peels were separated from the stalk and peeled, cut into smaller sizes and washed with deionised water to remove impurities present in the peels. This process was applied to all three species to ensure sample purity.

Production of Bio-Plastics from Banana Peels

The shredded banana peels were soaked in 0.5% $Na_2S_2O_5$ solution for five minutes in a 500 mL beaker before straining. The softened peels were transferred into a 2L beaker with sufficient water and boiled for 30 minutes. The resulting soft peels were blended using an electric kitchen blender until a homogeneous paste was formed. Excess water was removed using a fine cloth sieve. Approximately 30g of the sample pulp was placed in a 250 mL beaker, to which 3 mL of 0.5M HCl and NaOH solutions were added with continuous stirring. Additionally, 3 mL of propan-1,2,3-triol was incorporated with vigorous mixing. The resulting mixture was then spread evenly in a Petri dish and oven-dried at 130 °C for one hour. This experiment was repeated using varying concentrations of HCl while keeping the NaOH concentration constant at 0.5M. All experiments were conducted in triplicates. The produced bio-plastics were stored in a cool, dry place to prevent microbial infestation and excessive moisture loss.

Production of Bio-Plastics with Additives

Following the same procedure outlined in Section 3.2, varying percentages of iron rust and eggshell powder were incorporated into the mixture differently before adding the acid and base. Partial dissolution of the additives was observed, and thorough mixing ensured homogeneity.

Elemental Analysis

Dried, finely ground raw banana peels and bio-plastic samples were subjected to elemental analysis using the SKYRAY EDXRF spectrophotometer (Model EDX 3600B) at the Engineering Materials Development Institute, Akure, Nigeria.

Fourier Transform Infrared Spectroscopy (FTIR) Analysis

Sundried and pulverized banana peel samples, along with their corresponding bio-plastics, were analyzed using a SHIMADZU FTIR spectrophotometer (Model 8400S) at Redeemer's University, Ede.

Mechanical Testing

The bio-plastic samples were sundried, cut into rectangular specimens (3 × 1 cm), and subjected to mechanical testing at the Centre for Energy Research and Development (CERD), Obafemi Awolowo University, Ile-Ife. The tests were conducted using a computer-controlled Instron tensile testing machine (Model 3369) with a load capacity of 200N and a loading speed of 5 mm/s.

Water Absorption Test

The bio-plastics were cut into uniform sizes, weighed, and submerged in 100 mL of water in separate beakers. Their weights were recorded at six-hour intervals over 48 hours to assess water absorption.

Biodegradability Study

A biodegradability test was conducted to assess the degradation rate and the influence of additives. The experiment was carried out on fertile land near Moremi Hall, Obafemi Awolowo University. The soil was cleared of debris, tilled, and moistened before pre-weighed bio-plastic samples were buried in perforated containers at a depth of 0.5 feet. Samples were spaced 12 inches apart and labeled accordingly.

Environmental parameters at the time of burial included:

1. Temperature: 30°C – 33°C
2. Humidity: 82%
3. Visibility: 10 km
4. Atmospheric Pressure: 100.45 kPa
5. Cloud Cover: Mostly cloudy

Degradation was monitored weekly for five weeks by excavating and visually inspecting the samples. After removing adhering soil, their weights were measured using a digital balance. The burial site was divided into three sections for each species, with sub-sections assigned to different bio-plastic formulations (0.4M and 0.5M HCl, as well as formulations doped with 1.5% and 2% eggshell or iron rust). Burial was conducted after significant rainfall to ensure soil moisture.

Scanning Electron Microscopy (SEM)

A portion of the bio-plastic samples was subjected to SEM analysis at the Spectra Section, University of Johannesburg, South Africa. Samples were mounted on a copper grid, coated with a conductive carbon film, and examined using a VEGA 3 TESCAN electron microscope at 20 kV. Images were captured at various magnifications for detailed structural analysis.

Anion Analysis

Soil samples were collected from each burial section at uniform depths, sieved to remove coarse particles, and crushed into fine powder. 10 g of each soil sample was mixed with 100 mL of distilled water, shaken vigorously, and stored in pre-cleaned sample bottles for anion analysis. The concentration of selected anions in the soil was determined using standard analytical methods. This methodology ensures reproducibility and accuracy in the assessment of bio-plastics derived from banana peels, providing a comprehensive evaluation of their mechanical, environmental, and chemical properties.

RESULTS AND DISCUSSION

Table 1 represents the proximate composition of the three banana and plantain species: *Musa nana (Paranta), Musa paradisiaca (Agbagba), and Musa s. var. paradisiaca (Pambo).* Parameters including moisture content, ash, crude fibre, ether extract (fat), and crude protein were analysed. Among the three, *Musa nana* exhibited the highest values across all components, moisture (89.52%), ash (15.78%), crude fibre (7.28%), ether extract (8.53%), and crude protein (18.38%). This indicates that it is rich in nutrients and could possess significant dietary importance especially in terms of minerals, fibre and protein. On the other hand, *Musa paradisiaca, and Musa s. var. paradisiaca* exhibited lower values for the measured parameters, with *Musa s. var. paradisiaca* being the least overall.

Table 1: Proximate Composition of Selected Banana Species

Samples	Moisture (%)	Ash (%)	Crude Fibre (%)	Ether Extract (%)	Crude Protein (%)
Musa nana	89.52	15.78	7.28	8.53	18.38
Musa paradisiaca	83.48	11.51	5.46	6.85	12.03
Musa s.var.paradisiaca	83.09	10.66	4.41	5.41	12.03

Variation in Peel Percentage among Banana and Plantain Species

The percentage of peels obtained from the banana and plantain differ according to species. However, the results obtained were in agreement with several studies where they reported an average of 40% peels for various banana and plantain samples (Onojah & Emurotu, 2017; Palacios-Ponce et al., 2017). *Musa paradisiaca* had the largest percentage of peels due to its high fibrous nature while *Musa nana* had the lowest percentage. The results are presented in Table 2.

Table 2: Percentage of peels in the experimental samples

Samples	Yield (%)
Musa nana (Paranta)	45.82 ± 0.25
Musa paradisiaca (Agbagba)	65.78 ± 0.25
Musa Sapientum var paradisiaca (Pambo)	47.94 ± 0.25

Morphology of the Produced Bio-plastics

The bioplastics obtained were brownish in colour but leathery in nature (Figure 2). They exhibited the properties of a cellulosic fibre but with a slight difference due to the effect of the acid used in the production of the bio-plastics. They were very strong when in a semi-dry state. This could be attributed to the presence of secondary forces particularly hydrogen bonds and dipole interaction, in addition to the primary covalent bonds. On drying, the bioplastics were very hard and strong. This can be attributed to hornification, which induces tension in the region of the microfibrils causing molecular rearrangement; this disrupted and reformed the ordered region causing the strong texture of the bioplastics (Ferreira et al., 2014).

Figure 2: The produced Experimental Bioplastics

Elemental Analyses

The result of elemental analyses as presented in Table 3 showed the differences in concentration of elements present in eggshell (ES) and iron rust (IR) used as additives and those of the bio-plastics produced from the peel of *Musa nana* undoped and doped with both accelerators.

Some essential metals such as potassium, calcium, aluminum, chromium, copper, zinc, nickel, molybdenum, iron and manganese were present in substantial amount in the bio-plastic samples because of their significance in nutrition which include the control of heartbeat, regulation of blood (Jomova et al., 2022). These metals could also be involved in bond formation and cross linking enhancement which usually results in higher strength in their by-products. It was observed that the eggshell and bio-plastics gave significant amount of all the metals. The absence of Mg in the undoped bio-plastics was unexpected, but when doped with 2% eggshell, the concentration of Mg was found to be 1274 ppm. This could have been due to the displacement action of the Ca in the eggshell that pushed out the masked-Mg because it must have existed in trace quantities. Bio-plastics doped with eggshell were found to contain the highest concentration of Ca of 127,368 ppm than the one doped with iron rust which contained 9,746 ppm and the undoped with 48,525 ppm. Also, the bio-plastics doped with iron rust were found to contain the highest concentration of Fe of 205,511 ppm than the one doped with eggshell which contained 2881 ppm and the undoped with 3167 ppm. The increment in the calcium and iron content of the doped bio-plastics compared with the undoped ones might be due to the the summation experienced because they were added to the naturally existing ones in the experimental samples as buttressed in their elemental compositions. The reduction in Ca content of the bio-plastic doped with iron rust and also the decrease in the Fe content of the bio-plastic doped with eggshell might be attributed to the usage of more Ca and Fe ions respectively which resulted in a higher tensile strength. All the other metals present were found to have contributed to bond formation but the degree of involvement varies. Likewise, the possibility of the existence of associative forces most especially hydrogen bonding, dipole-dipole interactions and van-der Waals force is due to the polarity created by the presence of those metals within an organic system (Nohran *et al.,* 2013). The same trend was observed with bio-plastics made from *Musa paradisiaca* and *Musa s. var. paradisiaca*

Table 3: Elemental Composition of the Produced Bioplastics and Additives

Metal Composition	Eggshell	Iron rust	Bioplastics from *Musa nana*		
			0.5M HCl (ppm)	0.5M HCl + 2% ES (ppm)	0.5M HCl +2% IR (ppm)
Mg	1330 ± 0.0266	--	--	1274 ± 7	--
Al	1781 ± 5	4660 ± 23	6643 ± 34	7357 ± 4	5868 ± 3
Si	338 ± 3	10413±20	7490 ± 26	8813 ± 2	7406 ± 6
P	2535 ± 0.023	640 ± 36	3363 ± 30	6437 ± 5	3790 ± 3
S	3442 ± 6	--	21873 ±0.023	20334 ± 0.041	17792 ± 0.015
K	--	537 ± 31	55775 ± 0.012	58589±0.033	50934 ± 0.067
Ca	604696 ± 7	4471 ± 26	48525 ± 0.011	127368±0.012	9746 ± 4
Ti	--	--	--	--	--
V	62 ± 5	194 ± 28	49 ± 6	20 ± 4	71 ± 6
Cr	--	652 ± 23	9 ± 4	6 ± 2	166 ± 4
Mn	5 ± 3	2016±50	399 ± 8	247 ± 6	838 ± 7
Co	27 ± 6	--	9 ± 3	--	3290 ± 4
Fe	1921 ± 4	636716 ± 0.014	3167 ± 6	2881 ± 2	205511 ± 0.084
Ni	325 ± 7	515 ± 33	498 ± 9	476 ± 3	535 ± 6
Cu	238 ± 2	203 ± 36	725 ± 3	505 ± 4	512 ± 3
Zn	468 ± 1	369 ± 24	1241 ± 2	1043 ± 6	908 ± 4
W	222 ± 7	--	1473 ± 6	1333 ± 3	545 ± 2
Rb	8 ± 5	--	59 ± 4	17 ± 4	32 ± 4
Nb	--	--	211 ± 3	428 ± 2	96 ± 4
Mo	1971 ± 3	--	2025 ± 5	1873 ± 4	2094 ± 3
Sn	2795 ± 6	--	6959 ± 4	7002 ± 6	7382 ± 6
Sb	2454 ± 4	633 ± 20	5997 ± 6	6194 ± 4	5788 ± 4

LEGEND: IR – iron rust ES – egg shell

Fourier Transformed Infrared Spectroscopy

To ascertain the formation of bonds in the preparation of the bioplastics, the IR spectra of the fresh sample peels, IR spectra of the bioplastics without egg shell and iron, and IR spectra of the bioplastics containing egg shell and iron rust were analysed and compared. The spectra information is presented in Table 3-5 while the spectra are shown in Figure 2 (supplementary file).

The results revealed that bond formation took place via different functional groups as significant shift in the frequency of absorption were recorded. The characteristic functional groups observed in the banana and plantain peels includes C-O of acetals around 1246 cm^{-1}, O-H of lignocellulosic contents at 3400 cm^{-1}, C=O of amide at 1648 cm^{-1} and the 1525 cm^{-1} of aromatic C=C. The shifts in the stretching frequency of OH for the bioplastics revealed that bond formation occurred via the OH of the cellulosic content such as hemicellulose, lignin, and starch. The OH stretching frequency of the undoped *Musa nana* bio-plastics was observed at 3402 cm^{-1} while that of the doped *Musa nana* bioplastic was seen at 3295 cm^{-1}. Likewise, the OH stretching frequency of the undoped *Musa sapientum var. paradisiaca* bio-plastics was observed at 3402 cm^{-1} while that of the doped *Musa sapientum var. paradisiaca* bioplastic was seen at 3335 cm^{-1}. Furthermore, the OH stretching frequency of the undoped *Musa Musa paradisiaca* bio-plastics was observed at 3418 cm^{-1} while that of the doped *Musa paradisiaca* bioplastic was seen at 3289 cm^{-1}.

All doped species with 2% eggshell showed the same trend which involves bond formation through the –OH group. This could be as a result of the utilization of the lone pair of oxygen of the –OH in bond formation with the metal ions as provided by the electron deficient Fe^{3+} and Ca^{2+} ions provided by the iron rust and eggshell particles respectively. The disappearance of the -C=O stretch of ketone upon doping with 2% eggshell and 2% iron rust for the three species possibly suggested a transformation of the one π- plus one σ-electron bond system into a σ-bond system. Also, the carbonyl of the amide observed a decrease in absorption frequency upon doping. This could be as a result of the bond between the lone pair of oxygen and/or nitrogen of the amide with the Ca of the eggshell and Fe of Iron rust respectively, resulting in decrease in pie electron density and partial electron delocalization, which weakens the C=O bond shifting its absorption to a lower frequency.

Table 4: Infrared absorption band for fresh samples and their bioplastics (doped and undoped) with egg shell (cm^{-1})

Musa nana			Musa s.ver.paradisiaca			Musa paradisiaca			Tentative Assignment
Fresh peel	Bioplastic with 0.5M HCl	Bioplastic with 0.5M HCl +2% Iron rust	Fresh peel	Bioplastic with 0.5M HCl	Bioplastic with 0.5M HCl +2% Iron rust	Fresh Peel	Bioplastic with 0.5M HCl	Bioplastic with 0.5M HCl +2% Iron rust	
3410s,b	3402s,b	3295s,b	3427s,b	3402s,b	3335s,b	3410s,b	3418s,b		O-H stretch (inter- and intramolecular H-bonding
2926(m)	2942(m)	2921(m)	2926(m)	2942(m)		2926(m)	2926(m)	2927(m)	Saturated C-H symmetrical stretching
2344(w)	2344(w)	2162(w)	2357(w)	2353(w)		2369(w)	2353(w)	-	
2074(w)	2074(w)	2050(w)	2099(w)	2099(w)		2100(w)	2115(w)	-	
1721(w)	1729(w)		1754(w)	1800(w)					C=O stretch (ketone or aldehyde) /
1648(m)	1639(m)	1614(m)	1648(m)			1632(m)	1639(m)	1630(w)	C=O stretch (amide)
1525(w)	1541(w)		1598(w)	1525(w)	1596 (w)				C=C stretch (aromatics) / In-plane C-H bending
			1550(w)						
1443(w)	1450(w)		1393(w)	1425(w)		1393(w)	1410(w)	1375(w)	
1375(w)	1385(w)	1374(w)	1328(w)	1337(w)		1369(w)	1319(w)	-	
1328(w)	1350(w)								
1246(w)	1225(w)		1237(w)	1248(w)		1237(w)	1227(w)	-	C-O stretching (acetal)
1156(w)	1175(w)	1151(w)	1165(w)	1165(w)		1147(w)	1156(w)	1149(m)	
1075(w)	1115(w)		1075(w)	1080(w)		1074(w)	1033(m)	-	
1017(w)	1040(w)	1027(w)	1017(m)	1040(w)	1012(m)	1017(m)	-	1023(m)	
915(w)	927(w)	924(w)	925(w)	911(w)		911(w)	925(w)	-	C-C stretch (alkane)
836(w)	836(w)		845(w)	861(w)		861(w)	861(w)	-	

This might promote hydrogen bonding between the amide carbonyl and the surrounding carbonate and hydroxyl species, reducing the double bond character of C=O and thus lower its absorption frequency. Furthermore, the electronic environment of the amide could be altered by carbonates from the egg shells resulting in increased electron donation to C=O and a lower absorption frequency. It was observed that the –C-O stretch in the acetal functional group present in all the three species disappeared as a result of the formation of permanent bond between oxygen of acetal and the metal of the Eggshell and Iron rust respectively. Hence, the addition of natural accelerators such as eggshell and iron rust used in this work enhanced bond formation between the present functional group in the bio-plastics and the main metal.

Table 5: Infrared absorption band for fresh samples and their bioplastics (doped and undoped) with iron rust (cm^{-1})

Fresh Peel	Bioplastic with 0.5M HCl	Bioplastic with 0.5M HCl +2% Egg Shell	Fresh Peel (2)	Bioplastic with 0.5M HCl +2% Egg Shell	Bioplastic with 0.5M HCl +2% Egg Shell	Fresh Peel	Bioplastic with 0.5M HCl	Bioplastic with 0.5M HCl + 2% Egg Shell	Tentative Assignment
3410s,b	3402s,b	3307s,b	3427s,b	3402s,b	3294s,b	3410s,b	3418s,b	3296s,b	O-H stretch (inter- and intra-molecular H-bonding)
2926(m)	2942(m)	2920(m)	2926(m)	2942(m)	2922(m)	2926(m)	2926(m)	2921(m)	Saturated C-H symmetrical stretching
2344(w)	2344(w)	-	2357(w)	2352(w)	-	2369(w)	2353(w)	-	-
2074(w)	2074(w)	-	2099(w)	2099(w)	-	2100(w)	2115(w)	-	-
1721(w)	1729(w)	-	1754(w)	1800(w)	-				C=O stretch (ketone or aldehyde
1648(m)	1639(m)	1638(w)	-	1648(m)	1633(m)	1632(m)	1639(m)	1641(w)	C=O stretch of amide
1525(w)	1541(w)	-	1598(w)	1525(w)	-				C=C stretch (aromatics)
1443(w)	1450(w)	-	1550(w)	1425(w)	-	1393(w)	1410(w)	1376(w)	In place C-H bending
1375(w)	1385(w)	1373(w)	1328(w)	1337(w)	1375(w)	1369(w)	1319(w)	-	
1328(w)	1350(w)	-	-	-	-				
1246(w)	1225(w)	-	1237(w)	1248(w)	-	1237(w)	1227(w)	-	
1156(w)	1172(w)	1151(w)	1165(w)	1165(w)	-	1147(w)	1156(w)	-	C-O stretching (acetal)
1075(w)	1115(w)	1078(w)	1075(w)	1080(w)	1031(w)	1074(w)	1033(m)	1032(w)	
1017(w)	1040(m)	1021(w)	1017(m)	1040(m)	-	1017(m)	-	-	
915(w)	927(w)	-	925(w)	911(w)	-	911(w)	925(w)	-	C-C stretch (alkane)
836(w)	836(w)	-	845(w)	861(w)	3294s,b	861(w)	861(w)		

*b-broad; s- sharp; w- weak; m- medium

Scanning Electron Microscopy

The scanning electron micrographs of the prepared bioplastics, with and without additives, are presented in Figure 3a–g. At the same magnification (366×, Fig. 3a), the general surface morphology of all the bioplastics appeared very similar. The micrographs showed good interfacial bonding with a smooth appearance, indicating strong compatibility among the cellulosic starch granules in the pulp, glycerol, and the additives.

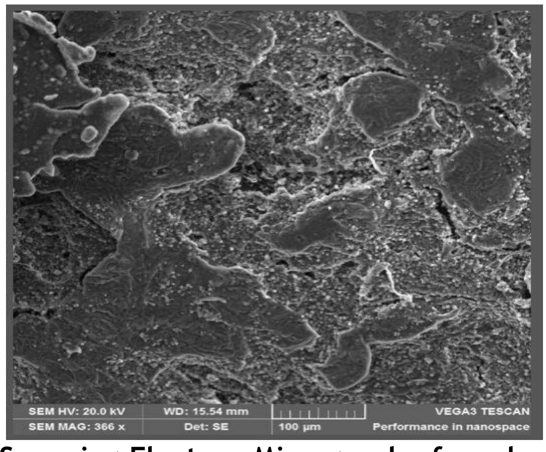

Figure 3-(a): Scanning Electron Micrograph of produced bioplastics

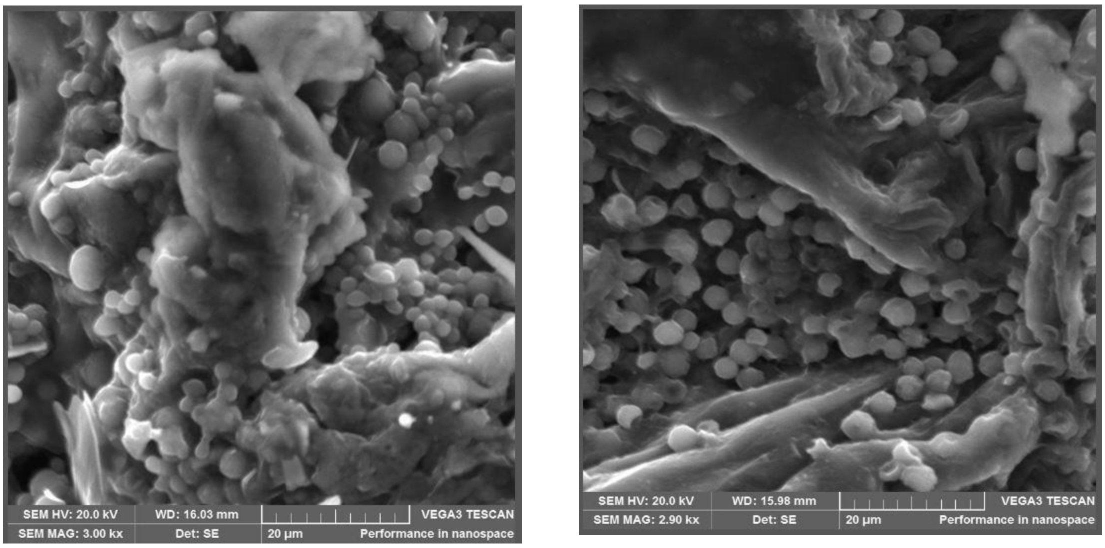

(b) (c)

Figure 3-(b) and (c): Microstructures from the SEM of *Musa nana* doped with iron rust and eggshell.

Similarly, the SEM microstructures of both doped and undoped samples revealed a uniform distribution of banana/plantain peel pulp particles within the bioplastic matrix. This uniformity can be attributed to strong bonding interactions among starch, water, and hydrochloric acid (HCl), which facilitated gelatinization and ultimately contributed to the formation of a solid structure. The HCl also played a role in releasing starch from the plant matrix (Ginting et al., 2017).

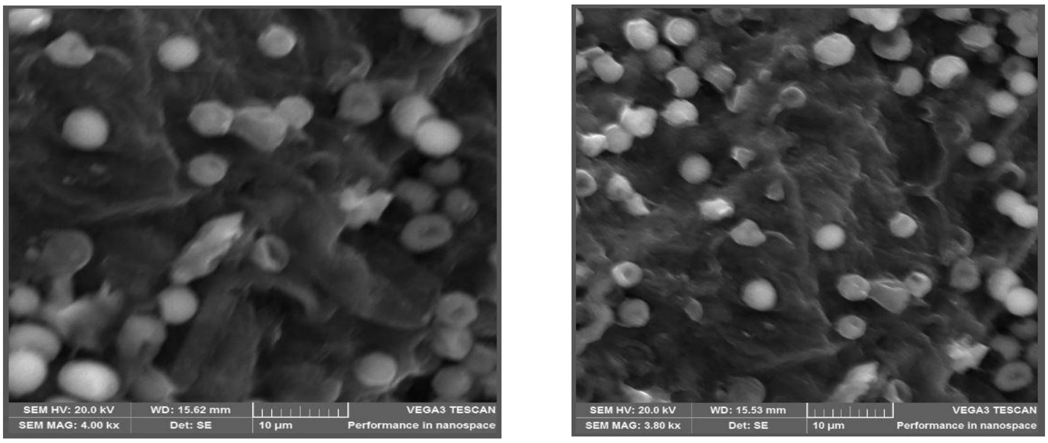

(d) (e)

Figure 3-(d) and (e): Microstructure from the Scanning Electron Micrograph of *Musa s. var. paradisiaca* doped with eggshell and iron rust.

Despite these similarities, distinct differences in lattice structure and molecular arrangements were observed in the crystalline cores of different samples, depending on the conditions under which they were produced. These differences were evident in the inter-packing interfaces. Figures 3b and 3c showed the microstructures of *Musa nana* samples doped with iron rust and eggshell, respectively, at the same magnification. The interfacial bonding in the rust-doped sample (Fig. 2b) appeared slightly stronger than in the eggshell-doped sample (Fig. 3c), possibly due to the higher moisture content and hydration capacity of Fe^{3+} ions, which could enhance hydrogen bonding within the bioplastic network.

The same trend was observed in the *Musa s. var. paradisiaca* but the difference observed was not as much as those seen in the *Musa nana* (Fig. 3d and e). The homogeneity observed was better than those in *Musa nana*. Because most of the banana pulp particles were assumed to be embedded in the amorphous matrix composed of randomly distributed ions.

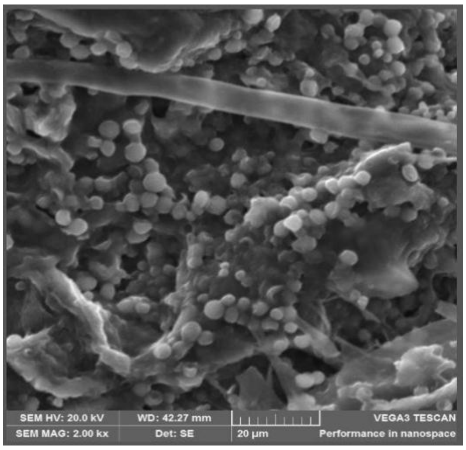

(f)

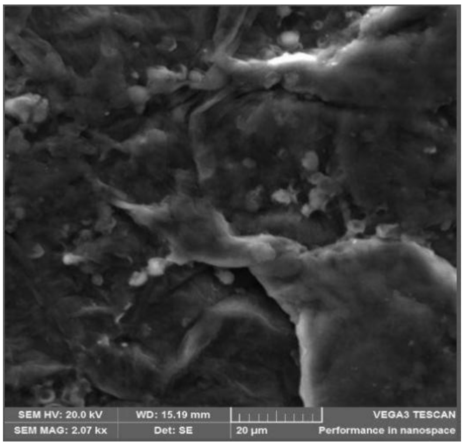

(g)

Figure 3-(f) and (g): Microstructure from the SEM of *Musa paradisiaca* doped with eggshell and iron rust.

Notably, a reverse trend was observed in the *Musa paradisiaca*-based bioplastics, where the eggshell-doped samples exhibited better interfacial bonding compared to those doped with iron rust. This behavior may be attributed to the relatively low fibre content of *Musa paradisiaca* peels, as indicated by the proximate analyses (Table 1), which likely enhances the matrix-filler interaction. Although direct evidence of metal ions breaking down lignin to release starch granules is limited, it is well established that metal ions interact with lignin and influence the structural behavior of lignocellulosic materials (Guo et al., 2008; Santander et al., 2021). In particular, alkaline earth metals like Ca^{2+}, present in eggshells, are more effective than transition metals such as Fe^{2+} in modifying fibre structure and enhancing interfacial bonding through cross-linking and structural rearrangement (Xu et al., 2025). This differential interaction might explain the improved performance of eggshell-doped *Musa paradisiaca* bioplastics.

Mechanical Performance

The mechanical properties of the bioplastics derived from *Musa paradisiaca*, *Musa sapientum var. paradisiaca*, and *Musa nana* were significantly influenced by the concentration of hydrochloric acid (HCl) used during processing, as well as by the type and amount of the doping agents (specifically egg shell and iron rust). Tensile strength, elongation at break, and Young's modulus were evaluated across various formulations, particularly focusing on two acid concentrations 0.4M and 0.5M HCl and doping agents including eggshell (ES) and iron rust (IR).

Tensile Strength

Figure 4 illustrated that higher tensile strength values were observed in bioplastics doped with eggshell and iron rust at both acid concentrations.

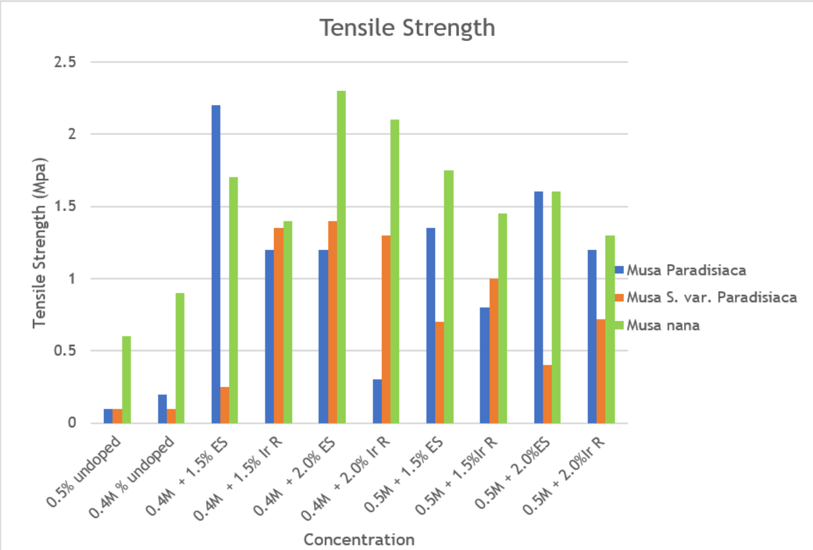

Figure 4: Variation of tensile strength with acid and additive concentrations of produced bioplastics

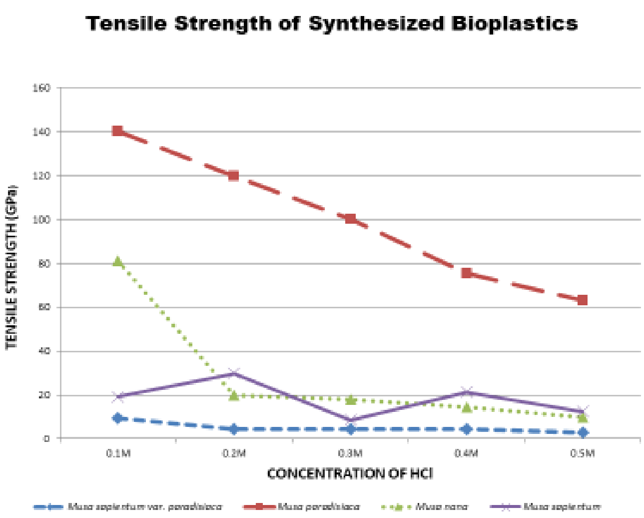

Figure 5: Effect of Additive Concentrations on the Tensile Strength of Synthesized Bioplastics

Overall, bioplastics incorporating eggshell demonstrated greater tensile strength compared to those containing iron rust. This difference can be attributed to the presence of calcium carbonate in eggshells, which is known for its high mechanical strength and stiffness. Additionally, calcium carbonate has been reported to act as a reinforcing filler in bioplastics. In contrast, the inclusion of iron rust particles appears to reduce the integrity of polymer chains, leading to a decrease in tensile strength. This may be due to the catalytic effect of iron rust, which can accelerate polymer degradation. Visually, the bioplastics containing iron rust appeared wet and moist, likely a result of the high hydration capacity and smaller ionic radius of Fe^{3+} compared to Ca^{2+}. This higher moisture content may also contribute to the reduced tensile strength observed in iron rust-doped bioplastics.

Among the samples, the bioplastic derived from *Musa nana* treated with 0.4 M HCl and doped with 2.0% eggshell exhibited the highest tensile strength. This suggests that higher acid concentrations may lead to a decline in tensile strength, likely due to over-hydrolysis, which compromises the integrity of the polymer chains.

Young's Modulus

The stiffness and elasticity of the bioplastics were assessed using Young's modulus, which followed a similar trend across the different samples. As shown in Figure 5, Bioplastic derived from *Musa nana* exhibited the highest modulus, followed by *Musa sapientum*, while *Musa paradisiaca* showed the lowest value. This variation suggests that, despite the botanical similarities among the samples, their cellulosic content differed significantly, as supported by the results of the proximate analysis (Table 1).

Bioplastics doped with eggshell showed a higher Young's modulus compared to those doped with iron rust. This difference can be attributed to the chemical nature of the metal ions involved.

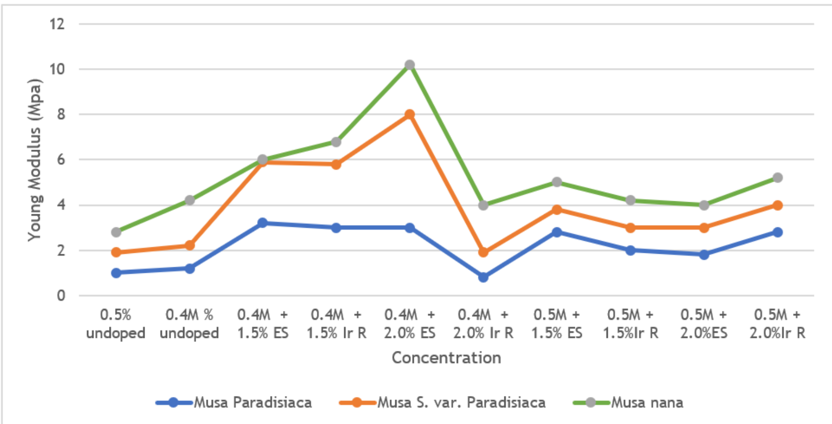

Figure 6: Variation of Young's modulus with acid and additive concentrations of the bioplastics

Eggshells provide calcium ions (Ca^{2+}), which form stable hydration shells and can chelate with functional groups in the polymer, creating strong physical crosslinks that enhance material stiffness. In contrast, iron ions (Fe^{3+}) from rust tend to hydrolyze and aggregate, resulting in poor dispersion and weaker interactions within the polymer matrix. Consequently, calcium from eggshells enhances the polymer network more effectively, leading to increased stiffness and a higher Young's modulus (Li et al., 2016; Sharif et al., 2023).

The highest Young's modulus was recorded in the bioplastic treated with 0.4 M HCl and doped with eggshell. This may be due to reduced cellulose crystallinity at that acid concentration, which favors better interaction between the polymer and the filler. In contrast, treatment with 0.5 M HCl led to a general decline in Young's modulus across all varieties of banana- and plantain-based bioplastics. This reduction is likely a result of over-hydrolysis of the starch matrix, which weakens the internal structure and diminishes the reinforcing effect of the fillers.

Elongation at Break

Elongation at break, a measure of bioplastic flexibility, exhibited an inverse relationship with tensile strength and Young's modulus across all samples. Bioplastics doped with either eggshell or iron rust showed higher elongation compared to their undoped counterparts. Notably, bioplastics containing iron rust generally demonstrated greater elongation than those doped with eggshell, indicating enhanced flexibility but compromised mechanical integrity. Figure 6 showed the elongation at break for the produced bioplastics.

Among the samples, bioplastics derived from *Musa paradisiaca*, particularly those without reinforcement or doped with iron rust, exhibited the highest elongation percentages. This highlights their superior flexibility but lower mechanical strength. In contrast, the most rigid bioplastics were those treated with 0.4 M HCl and doped with eggshell, which showed significantly reduced elongation. This finding confirms the common trade-off in material properties, where increased strength and stiffness often result in decreased flexibility (Hashim et al., 2024; Li et al., 2016).

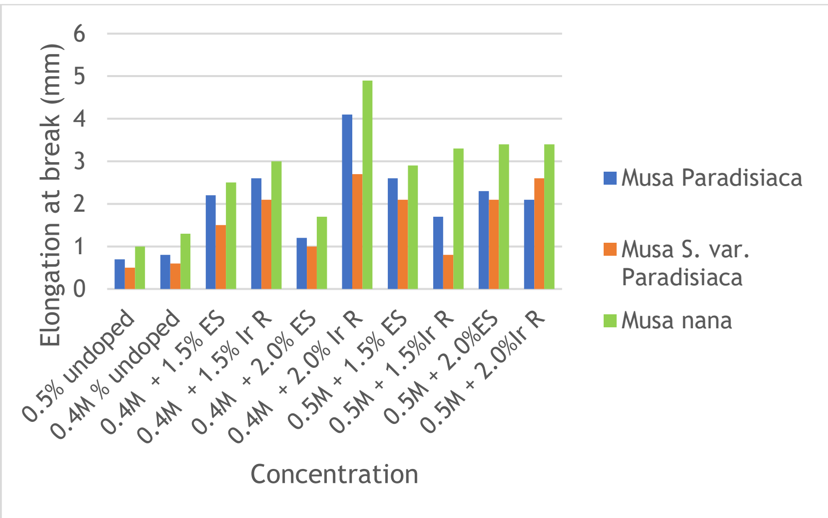

Figure 7: Variation of elongation at break with acid and additive concentrations of produced bioplastics

Water Absorption

Figures 7-9 displayed the water absorption capacities of bioplastics doped with eggshell (ES) and iron rust (IR) at two different acid concentrations. Across all varieties and treatment conditions, water absorption increased over time, reaching a plateau around 36 to 42 hours. Additionally, bioplastics doped with 2.0% additives absorbed more water than those doped with 1.5%. Treatment with 0.5 M HCl consistently resulted in higher water absorption compared to 0.4 M HCl, except for bioplastics derived from *Musa paradisiaca*. This suggested that stronger acid hydrolysis may increase the porosity or hydrophilicity of the material.

Among the varieties tested, bioplastics derived from *Musa paradisiaca* exhibited the highest overall water absorption. Within this group, eggshell-doped samples absorbed significantly more water than those doped with iron rust, especially at the 2.0% concentration. This is likely due to increased pore formation or enhanced hydrophilicity imparted by the calcium carbonate ($CaCO_3$) present in eggshells. The data also showed that water absorption in most samples plateaued after 30 to 36 hours, indicating the bioplastics had reached saturation.

Bioplastics derived from *Musa nana* demonstrated moderate water absorption compared to the other samples. Unlike *Musa paradisiaca*, the difference between eggshell and iron rust doping was less pronounced, and water uptake was more gradual and steady, possibly reflecting a denser or less porous polymer matrix. Similarly, bioplastics derived from *Musa sapientum* var. *paradisiaca* followed trends comparable to *Musa nana*, with the highest absorption observed in samples doped with 2.0% eggshell and treated with 0.5 M HCl.

Overall, eggshell consistently promoted greater water uptake than iron rust. This difference may be attributed to the presence of $CaCO_3$ in eggshells, which can create a rougher surface morphology and higher porosity. Conversely, the lower absorption observed in iron rust-doped bioplastics may result from fewer polar interactions within the polymer matrix.

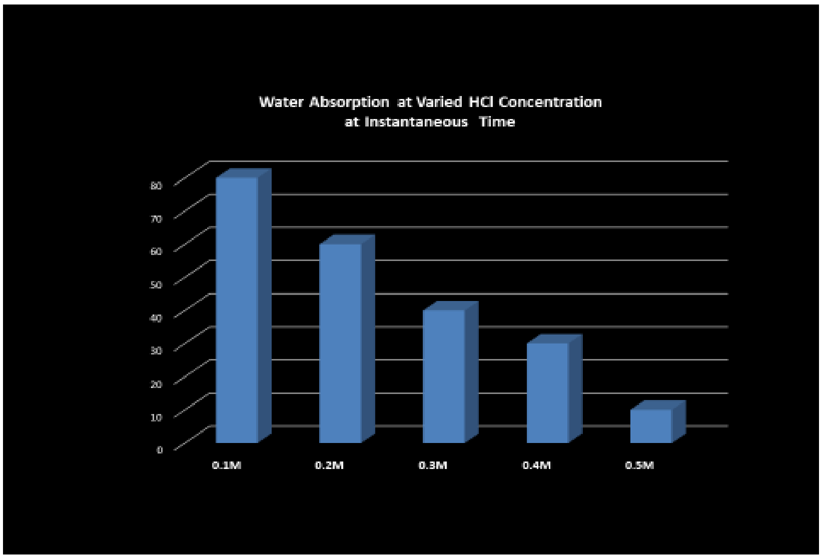

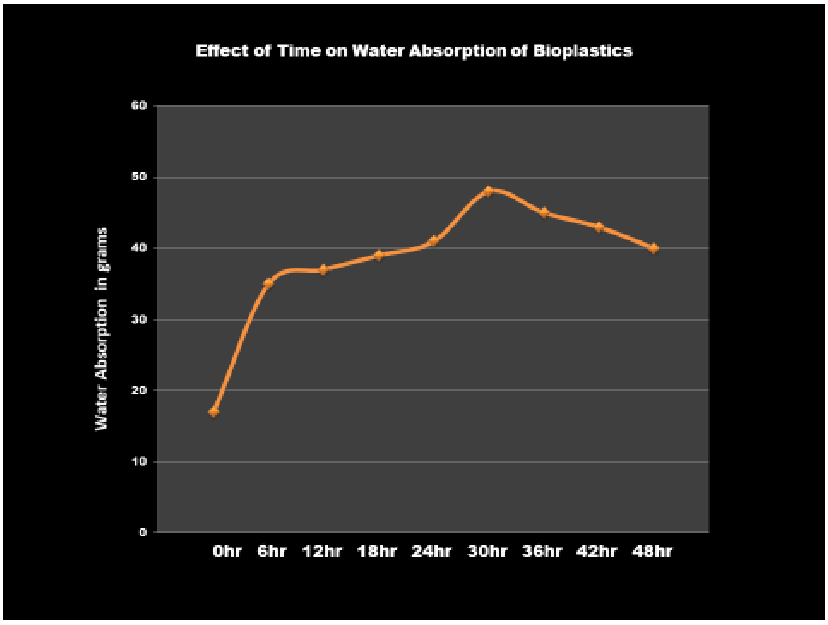

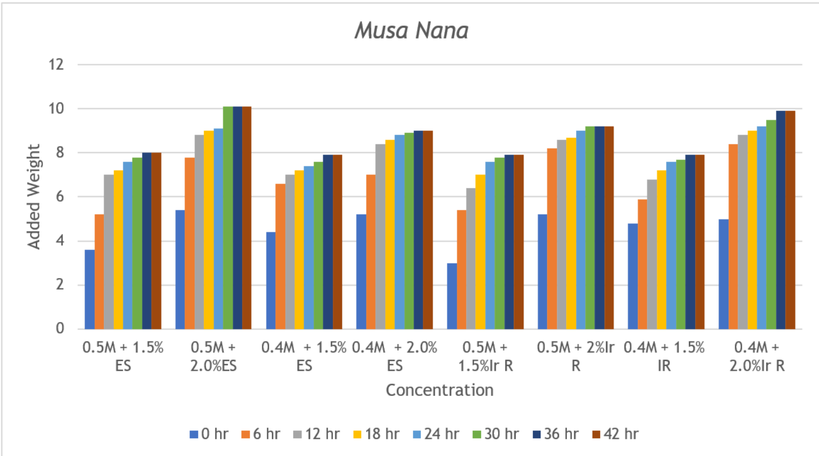

Figure 8: Water absorption of bioplastics from *Musa nana* with additives

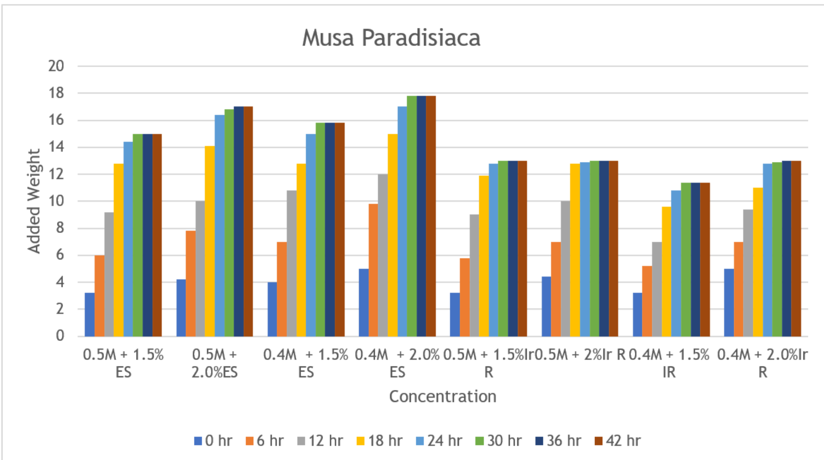

Figure 9: Water absorption of bioplastics from *Musa Paradisiaca* with additives

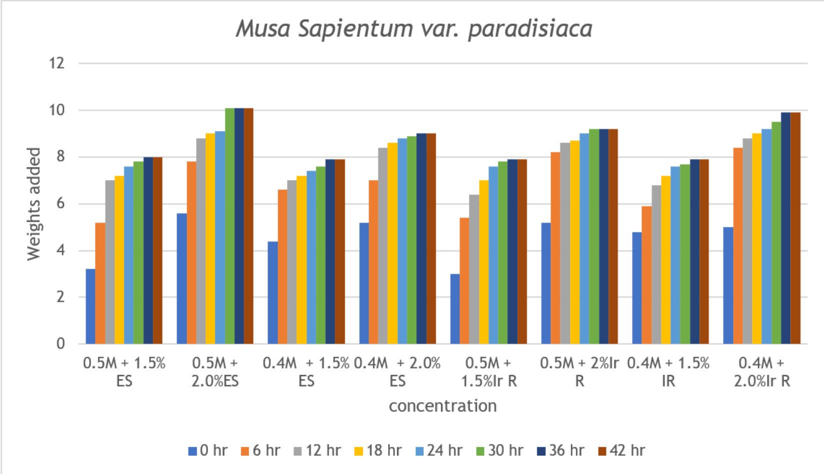

Figure 10: Water absorption of bioplastics from *Musa Sapientum var. paradisiaca* with additives

Biodegradation

As shown in Figure 10-12, rate of biodegradation vary among the different bioplastics produced, with their composition playing a significant role in the process. All bioplastics fully degraded by the third or fourth week, confirming their biodegradability. In the first week, no noticeable degradation occurred; instead, all buried samples gained weight due to moisture absorption from the soil. This is expected, as microbial and bacterial activities require moisture to thrive. Studies indicate that optimal bacterial activity occurs when the soil moisture content is between 50 – 70% of the water holding capacity of the soil (Bian et al., 2022).

Overall, the rate of biodegradation increased over time. A sharp weight loss observed in the later weeks signaled the onset of significant microbial degradation. Bioplastics treated with 0.5 M HCl degraded faster than those treated with 0.4 M HCl, likely due to the stronger acid weakening the polymer matrix more extensively. In contrast, bioplastics treated with 0.4 M HCl showed a more gradual degradation pattern, suggesting greater structural stability while still ensuring complete biodegradability. Among the different varieties, bioplastics derived from *Musa paradisiaca* exhibited the highest degradation rate, particularly those treated with 0.5 M HCl and doped with iron rust (IR), which were completely degraded by the third week. This was followed by bioplastics from *Musa sapientum,* while those derived from *Musa nana* demonstrated the slowest biodegradation rate (Figures 4–6). Within *Musa paradisiaca*-based bioplastics, samples doped with IR degraded slightly faster than those doped with eggshell (ES).

In general, IR accelerated degradation more effectively than ES, especially in bioplastics treated with 0.5 M HCl. This may be attributed to the oxidative properties of iron rust, which can promote polymer chain scission. On the other hand, eggshell (ES) provided calcium carbonate, which may initially slow microbial activity by creating a more stable polymer matrix or less favorable conditions for microbial colonization. However, calcium carbonate eventually degrades, allowing microbial action to proceed. Thus, while ES may delay the onset of degradation, it does not prevent full biodegradation and may contribute to a more controlled and sustained breakdown of the bioplastic over time.

a b

<u>Figure 11-(a) and (b)</u>: **Biodegradation Experimental Sample bottles and Sample burial site for Biodegradation Test**

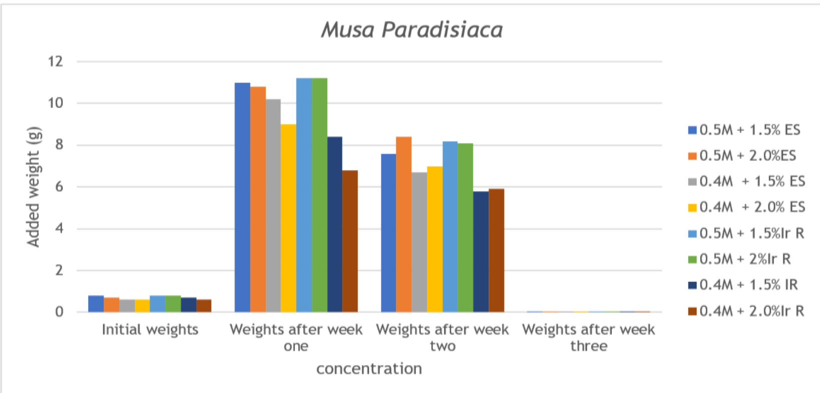

<u>Figure 12</u>: **Biodegradation of bioplastics produced from the peels of *Musa paradisiaca* doped with egg shell and rust**

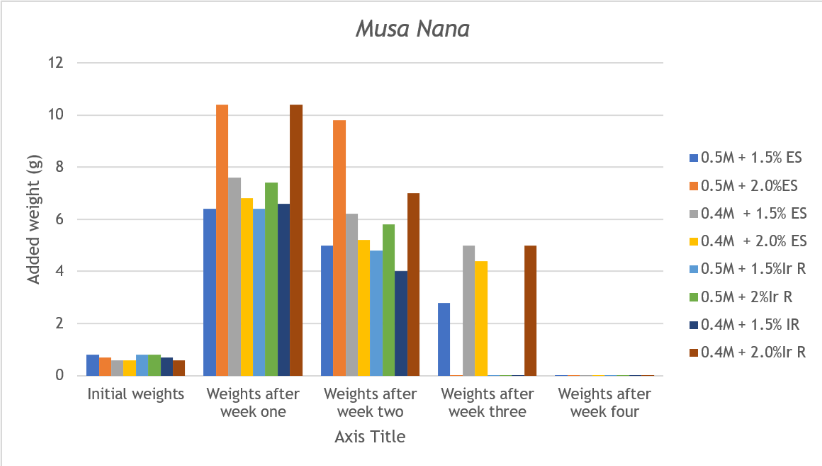

<u>Figure 13</u>: Biodegradation of bioplastics produced from the peels of *Musa nana* doped with egg shell and rust

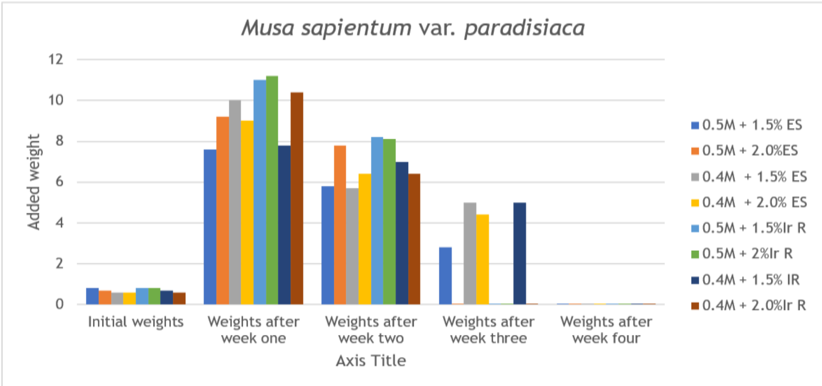

<u>Figure 14</u>: Biodegradation of bioplastics produced from the peels of *Musa sapientum var. paradisiaca* doped with eggshell and rust

Effect of Soil Composition on Biodegradation

Soil composition plays a critical role in microbial activity and, consequently, in the biodegradation of bioplastics. Both the cationic and anionic content of soil influence microbial metabolism, enzyme function, and the chemical environment in which degradation occur (Zhou et al., 2024). While some metal cations can inhibit microbial activity by binding to enzyme active sites, anions affect the soil pH, which directly impacts the rate of biodegradation.

Analysis of the anions present in the experimental biodegradation site (Table 6) revealed elevated concentrations of chloride (Cl^-), bicarbonate (HCO_3^-), and carbonate (CO_3^{2-}), along with moderate levels of sulfate (SO_4^{2-}) and nitrate (NO_3^-). These dissolved anions likely created a mildly acidic to neutral soil environment, which would be expected to influence microbial dynamics. Although microbial activity generally thrives within a pH range of 6 to 8, even slight deviations from this optimal range, such as those caused by excess chloride or bicarbonate, can reduce enzymatic efficiency and slow degradation.

This finding aligns with the experimental results, where initial degradation was slow and significant weight loss was only observed in the later weeks. The acidic nature of the soil, possibly influenced by the accumulation of acidic anions like chloride and nitrate, may have delayed the onset of microbial activity, leading to the gradual and non-spontaneous degradation pattern observed. This observation is consistent with the report by Famiglietti et al. (2025) and Kaur & Chauhan (2024) who noted that low pH conditions can hinder microbial action. Additionally, soil composition influences the mobility and availability of both anions and cations, which may adsorb onto the bioplastic surfaces (Chah et al., 2022; Famiglietti et al., 2025). These interactions can affect the surface chemistry and porosity of the bioplastics, as well as their susceptibility to microbial colonization and enzymatic (Kaur & Chauhan, 2024). For example, negatively charged anions may reduce the binding efficiency of positively charged microbial enzymes to the bioplastic matrix, thereby modulating the degradation rate.

Table 6: Anions from the biodegradation experimental site

Anions	Concentration (mg/L)
Cl^-	125.92 ± 0.068
HCO^{3-}	116 ± 0.034
$CO3^{2-}$	32 ± 0.041
$SO4^{2-}$	16 ± 0.021
$NO3^-$	6.18 ± 0.042

CONCLUSION

In conclusion, *Musa nana* and *Musa paradisiaca* peels are effective feedstocks for bioplastic production, especially when enhanced with eggshell and iron rust additives. Eggshell significantly improved tensile strength and stiffness due to its calcium carbonate content, while iron rust increased flexibility and accelerated biodegradation, likely because of its oxidative properties.

Structural and elemental analyses confirmed good dispersion, interfacial bonding, and the incorporation of essential metals. FTIR revealed molecular interactions through hydroxyl and carbonyl groups, and SEM supported homogeneous additive distribution. The best mechanical performance was observed with 0.4M HCl and eggshell, while higher HCl concentrations displayed reduced strength, possibly due to over-hydrolysis.

All bioplastics fully degraded within 3 to 4 weeks, with iron rust and acidic conditions accelerating the process. Soil anions such as chloride and bicarbonate influenced degradation rates by altering microbial activity and pH. These agro-waste-derived bioplastics, enhanced with natural additives, show strong potential as sustainable alternatives to conventional plastics.

REFERENCES

Abu Ubaidah, A. S., Mohamad Puad, N. I., Hamzah, F., Azmi, A. S., & Ahmad Nor, Y. (2024). Synthesis of bioplastics and the effects of additives on the mechanical, thermal and biodegradable properties. *Polymers from Renewable Resources*, *15*(4), 430–490.

Alcivar-Gavilanes, M. G., Carrillo-Anchundia, K. L., & Rieral, M. A. (2022). Development of a bioplastic from banana peel. *Ingeniería e Investigación*, *42*(3), 202

Ansari, N. A. I. M., Ramly, N., Faujan, N. H., & Arifin, N. (2023). Nutritional content and bioactive compounds of banana peel and its potential utilization: A review. *Malaysian Journal of Science Health & Technology*, *9*(1), 74–86.

Ataeian, P., Trinh, B. M., & Mekonnen, T. H. (2024). Effect of pro-oxidants on the aerobic biodegradation, disintegration, and physio-mechanical properties of compostable polymers. *Journal of Applied Polymer Science*, *141*(8), e54970.

Azieyanti, N. A., Amirul, A., Othman, S. Z., & Misran, H. (2020). Mechanical and morphology studies of bioplastic-based banana peels. *Journal of Physics: Conference Series*, *1529*(3), 032091.

Bian, H., Li, C., Zhu, J., Xu, L., Li, M., Zheng, S., & He, N. (2022). Soil moisture affects the rapid response of microbes to labile organic C addition. *Frontiers in Ecology and Evolution*, *10*, 857185.

Chah, C. N., Banerjee, A., Gadi, V. K., Sekharan, S., & Katiyar, V. (2022). A systematic review on bioplastic-soil interaction: Exploring the effects of residual bioplastics on the soil geoenvironment. *Science of the Total Environment*, *851*, 158311.

Dalimunthe, N. F., Ambarita, E. D., Barus, L. E., & Hanief, S. (2024). Characterization of a bioplastic spoon based on kepok banana (Musa acuminata balbisiana C.) starch with the addition of areca nut shells (Areca catechu L.) and glycerol. *IOP Conference Series: Earth and Environmental Science*, *1352*(1), 012009.

Desidery, L., & Lanotte, M. (2022). Polymers and plastics: Types, properties, and manufacturing. In *Plastic waste for sustainable asphalt roads* (pp. 3–28). Elsevier.

Emadian, S. M., Onay, T. T., & Demirel, B. (2017). Biodegradation of bioplastics in natural environments. *Waste Management*, *59*, 526–536.

Famiglietti, M., Mirpoor, S. F., Caporale, A. G., Cappelli, C., Tarallo, O., & Mariniello, L. (2025). Hydrocolloid-based bioplastics: Degradation in characterized soils. *International Journal of Biological Macromolecules*, *284*, 137988.

Ferreira, S. R., Lima, P. R. L., Silva, F. A., & Toledo Filho, R. D. (2014). Effect of sisal fiber hornification on the fiber-matrix bonding characteristics and bending behavior of cement based composites. *Key Engineering Materials*, *600*, 421–432.

Folino, A., Karageorgiou, A., Calabrò, P. S., & Komilis, D. (2020). Biodegradation of wasted bioplastics in natural and industrial environments: A review. *Sustainability*, *12*(15), 6030.

George, S. (2020). Plastics we cannot live without. In *Plastic Waste and Recycling* (pp. 449–466). Elsevier. https://www.sciencedirect.com/science/article/pii/B9780128178805000177

Ghaffar, I., Rashid, M., Akmal, M., & Hussain, A. (2022). Plastics in the environment as potential threat to life: An overview. *Environmental Science and Pollution Research*, *29*(38), 56928–56947.

Ginting, M. H. S., Hasibuan, R., Lubis, M., Tanjung, D. S., & Iqbal, N. (2017). Effect of hydrochloric acid concentration as chitosan solvent on mechanical properties of bioplastics from durian seed starch (Durio zibethinus) with filler chitosan and plasticizer sorbitol. *IOP Conference Series: Materials Science and Engineering*, *180*(1), 012126.

Gressler, S., Prenner, S., Kurz, A., Resch, S., Pavlicek, A., & Part, F. (2020). Polymer Nanocomposites—Additives, Properties, Applications, Environmental Aspects. *Green Sustainable Process for Chemical and Environmental Engineering and Science*, 331–358.

Guo, X., Zhang, S., & Shan, X. (2008). Adsorption of metal ions on lignin. *Journal of Hazardous Materials*, *151*(1), 134–142.

Hashim, F., Zabri, A. H., Ismail, N. H. C., Din, S. N., & Zaini, N. A. M. (2024). The Effect of Eggshell Powder (ESP) Filler on the Properties of Purple Sweet Potato (PSP) Starch Bioplastics. *Scientific Research Journal*, *21*(1), 117–131.

Hassan, T. A., Rangari, V. K., & Jeelani, S. (2014). Value-Added Biopolymer Nanocomposites from Waste Eggshell-Based $CaCO_3$ Nanoparticles as Fillers. *ACS Sustainable Chemistry & Engineering*, *2*(4), 706–717.

Homavand, A., Cree, D. E., & Wilson, L. D. (2024). Polylactic acid composites reinforced with eggshell/CaCO3 filler particles: A review. *Waste*, *2*(2), 169–185.

Huzaisham, N. A., & Marsi, N. (2020). Utilization of banana (Musa paradisiaca) peel as bioplastic for planting bag application. *International Journal of Advanced Research in Engineering and Technology (IJARET)*, *11*(4).

Jomova, K., Makova, M., Alomar, S. Y., Alwasel, S. H., Nepovimova, E., Kuca, K., Rhodes, C. J., & Valko, M. (2022). Essential metals in health and disease. *Chemico-Biological Interactions*, *367*, 110173.

Kasmuri, N., & Zait, M. S. A. (2018). Enhancement of bio-plastic using eggshells and chitosan on potato starch based. *Int. J. Eng. Technol*, *7*(3), 110–115.

Kaur, R., & Chauhan, I. (2024). Biodegradable plastics: Mechanisms of degradation and generated bio microplastic impact on soil health. *Biodegradation*, *35*(6), 863–892.

Kumar, S., Patel, D. K., Sharma, H. O., & Kumar, S. R. (2024). Eggshells Utilisation in Polymer Composites. *Key Engineering Materials*, *981*, 143–150.

Li, Y., Xin, S., Bian, Y., Xu, K., Han, C., & Dong, L. (2016). The physical properties of poly (L-lactide) and functionalized eggshell powder composites. *International Journal of Biological Macromolecules*, *85*, 63–73.

Maura, C. S., Athariq, M., & Mulmeyda, R. (2024). Utilization of Plantain Peel (Musa sapientum) and Sweet Potato Starch (Ipomea batatas) Waste in Combination with Glycerol Addition to Produce Biodegradable Plastic. *Chemistry and Materials*, *3*(2), 50–55.

Muthusamy, M. S., & Pramasivam, S. (2019). Bioplastics–an eco-friendly alternative to petrochemical plastics. *Current World Environment*, *14*(1), 49.

Onojah, P. K., & Emurotu, J. E. (2017). Phytochemical screening, proximate analysis and mineral composition of riped and unriped Musa species grown in Anyigba and its environs. *Inter J Res Agric Sci*, *4*, 2348–3997.

Palacios-Ponce, S., Ilyina, A., Ramos-González, R., Ruiz, H. A., Martínez-Hernández, J. L., Segura-Ceniceros, E. P., Aguilar, M. A., Sánchez, O., & Aguilar, C. N. (2017). Bioproducts obtained from the bioprocessing of the banana peel waste: An Overview. *Applied Chemistry and Chemical Engineering, Volume 5*, 223–250.

Pooja, N., Chakraborty, I., Rahman, Md. H., & Mazumder, N. (2023). An insight on sources and biodegradation of bioplastics: A review. *3 Biotech*, *13*(7), 220.

Razak, N. I. A., Abd Munir, H. M., Hashim, F., Norizan, M. N., Razali, N., & Kassim, M. H. M. (2024). Exploring the Cellulose Content on the Thermal and Mechanical Properties of Banana Peel Blend Tapioca Starch Bioplastic. *PaperASIA*, *40*(6b), 123–134.

Rosenboom, J.-G., Langer, R., & Traverso, G. (2022). Bioplastics for a circular economy. *Nature Reviews Materials*, *7*(2), 117–137.

Santander, P., Butter, B., Oyarce, E., Yáñez, M., Xiao, L.-P., & Sánchez, J. (2021). Lignin-based adsorbent materials for metal ion removal from wastewater: A review. *Industrial Crops and Products*, *167*, 113510. https://doi.org/10.1016/j.indcrop.2021.113510

Senthil, J., & Madan, R. P. (2015). Preparation and characterization of reinforced egg shell polymer composites. *International Journal on Mechanical Engineering and Robotics*, *3*(3), 7–17.

Sharif, N., Mohanta, M., & Thirugnanam, A. (2023). Eggshell reinforced yam starch-based bioplastic for packaging applications. *Journal of Packaging Technology and Research*, *7*(2), 75–86.

Sharma, S., Sharma, V., & Chatterjee, S. (2023). Contribution of Plastic and Mcroplastic to Global Climate Change and their Conjoining Impacts on the Environment-A review. *Science of the Total Environment*, *875*, 162627.

Tsado, A. N., Okoli, N. R., Jiya, A. G., Gana, D., Saidu, B., Zubairu, R., & Salihu, I. Z. (2021). Proximate, Minerals, and Amino acid Compositions of Banana and Plantain Peels. *BIOMED Natural and Applied Science*, *1*(01), 032–042.

Wang, M., Wen, J., Huang, Y., & Hu, P. (2021). Selective Degradation of Styrene-Related Plastics Catalyzed by Iron under Visible Light. *ChemSusChem*, *14*(22), 5049–5056.

Xu, Y., Li, C., Yang, S., Wang, S., Li, M., Jin, J., Jiang, Z., & Peng, F. (2025). Metal Ion Cross-Linked Cellulose/Lignin Nanocomposite Films: A Pathbreaking Approach toward High-Performance Sustainable Biomaterials. *ACS Nano*, *19*(10), 9801–9813.

Zhou, A., Ji, Q., Kong, X., Zhu, F., Meng, H., Li, S., & He, H. (2024). Response of Soil Property and Microbial Community to Biodegradable Microplastics, Conventional Microplastics and Straw Residue. *Applied Soil Ecology*, *196*, 105302.